Green Chemistry

PAPER

View Article Online
View Journal | View Issue

Cite this: *Green Chem.*, 2025, **27**, 8649

Green synthesis of scalable non-soluble hydrogels: rapid transesterification of maltodextrin with dimethylcarbonate using DABCO/DMSO†

Mohamed M. H. Desoky, *[a,b] Gjylije Hoti, [a,d] Arshak Tsaturyan, [c] Claudio Cecone, [a] Fabrizo Caldera[a] and Francesco Trotta[a]

Received 29th April 2025,
Accepted 20th June 2025

DOI: 10.1039/d5gc02156a

rsc.li/greenchem

This study presents novel synthetic approaches and catalysts to improve selectivity and energy efficiency, leveraging renewable feedstocks. Hydrogels, valued for their dynamic composition and versatile three-dimensional structure, hold significant promise in controlled release systems. Our investigation focuses on the synthesis of water-insoluble crosslinked hydrogels, particularly maltodextrin-based polymers, guided by green chemistry principles. Utilizing organocatalysis, notably 1,4-diazabicyclo[2.2.2]octane, and dimethylcarbonate as environmentally friendly alternatives, we demonstrate a synthesis pathway that minimizes waste and hazardous byproducts. This work aligns with the tenets of green chemistry, promoting sustainable chemistry practices while mitigating environmental impact.

Green foundation

1. Advancing green chemistry: our work pioneers a sustainable synthesis of maltodextrin-based hydrogels by replacing toxic phosgene and harsh reagents with dimethyl carbonate (DMC) as a crosslinker, DABCO as an eco-friendly catalyst, and DMSO as a greener solvent. This one-pot process minimizes waste and energy consumption while using reagents with reduced environmental impact.
2. Green chemistry achievement: the method achieves an ~80% yield under mild conditions (70–110 °C) and produces hydrogels with high water absorption (up to 549%) and tunable cross-linking densities, as verified by Flory–Rehner theory and rheological measurements—demonstrating both qualitative and quantitative green benefits.
3. Further greening opportunities: future research could enhance sustainability by replacing the homogeneous DABCO catalyst with a heterogeneous alternative. For instance, this might involve supporting an organocatalyst on glass beads to improve recyclability and reduce waste.

Introduction

From a vantage point of global sustainability, there has been a discernible trend towards the development of innovative synthetic methodologies and catalysts aimed at bolstering both selectivity and energy efficiency. This paradigm shift, when coupled with a transition towards utilizing renewable feedstocks, represents a pivotal strategy in the pursuit of designing environmentally benign commodity chemicals and monomers.[1] Moreover, hydrogels have emerged as prominent subjects of scientific inquiry, particularly in the realm of controlled release systems, owing to their dynamic chemical composition and intricate three-dimensional architecture. Endowed with exceptional mechanical resilience, augmented water content, and innate biocompatibility, hydrogels represent a compelling frontier in modern chemistry research.[2,3] Furthermore, water-insoluble substances housing amorphous solid dispersions (ASDs) represent a burgeoning class of pharmaceutical vehicles poised to enhance the dissolution kinetics and solubility kinetics of inadequately soluble medications. ASDs constructed upon water-insoluble crosslinked hydrogels exhibit distinctive attributes compared to those formulated on traditional water-soluble and water-insoluble matrices.[4] Additionally, hydrophilic polymer networks with a three-dimensional structure and the capacity to absorb sizable volumes of water are referred to as hydrogels. They exhibit a high level of biocompatibility and have a high degree of tissue resemblance, enabling a controlled and beneficial interaction with biological systems.[5] Because of this, hydrogels are now widely used in a variety of industries, including the bio-

[a]*Department of Chemistry, University of Torino, Via P. Giuria 7, 10125 Torino, Italy. E-mail: mohmed.desoky@gmail.com, mohamed.desoky@unipd.it*
[b]*Department of Chemistry, University of Padova, Via F. Marzolo 1, 35122 Padova, Italy*
[c]*Institute of Physical and Organic Chemistry, Southern Federal University, 194/2, Stachka Ave., Rostov-on-Don, 344090, Russia*
[d]*Department of Drug Science and Technology, Via P. Giuria 9, 10125 Torino, Italy*
† Electronic supplementary information (ESI) available. See DOI: https://doi.org/10.1039/d5gc02156a

medical, biotechnological, and pharmaceutical sectors.[6–12] Hydrogels are appealing platforms for the regulated release of medicinal substances and act as scaffolds in tissue engineering to assist and improve tissue regeneration.[13–15] Crosslinking techniques represent a widely employed method for synthesizing insoluble hydrogels from soluble polymers. This approach enables the hydrogel to maintain its structural integrity while stretching and absorbing water. By precisely adjusting the ratio of polymer to crosslinker, the resulting hydrogel's characteristics, such as size and entrapment efficiency, can be finely tuned, providing meticulous control over its properties.[16] Linear polysaccharides, such as maltodextrins (MDs), have found extensive applications in the pharmaceutical industry as encapsulating agents, excipients, and film-forming water-soluble polymers. Moreover, they are used in the food industry in products such as sports drinks and quick energy satchels.[17,18] As, MDs, stemming from starch degradation, boast beneficial traits like ample functional groups, cost-effectiveness, non-toxicity, and eco-friendliness, ideal for sample prep. However, their high solubility in water poses a challenge to direct application. Indeed, the synthesis presented in this study represents a pioneering approach, showcasing the application of sustainable green chemistry principles. In addition, in green chemistry, organocatalysis has surged in popularity, thanks to its efficiency and selectivity. Among the catalysts, 1,4-diazabicyclo[2.2.2]octane shines as a non-toxic, highly reactive, eco-friendly, and cost-effective option. Studies confirm its ability to deliver excellent yields with exceptional selectivity, marking a significant advancement in sustainable chemistry.[19–23] This work achieves synthesis pathway for maltodextrin hydrogel by minimized waste generation and hazardous byproducts Scheme 1.

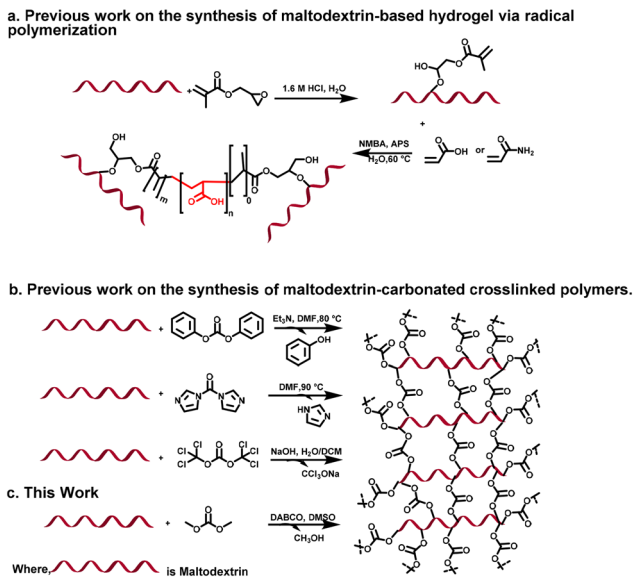

Scheme 1 Routes for maltodextrin cross linked polymers and hydrogels.

Experiments and materials

Materials

Maltodextrin Glucidex 2® (GLU2) was sourced from Roquette Freres (Lestrem, France), while 1,4-diazabicyclo[2.2.2]octane (DABCO), dimethyl sulfoxide (DMSO), and solvents were procured from Sigma-Aldrich (Darmstadt, Germany). Prior to use, GLU2 underwent thorough drying in an oven at 75 °C until reaching a constant weight.

Methods

Synthesis procedure of the hydrogel. In a round-bottom flask connected with reflux condenser, 10 g of GLU2 (55.5 mmol, 1 eq.) were dissolved in 30 mL of DMSO. DABCO (from 0 to 1.8 mmol) was then added to the solution. Subsequently, 10 mL of dimethyl carbonate (DMC) (118.8 mmol, 2.15 eq.) was introduced into the mixture. The reaction mixture was heated to 70, 85, or 110 °C until the formation of a non-soluble hydrogel occurred, which was then cooled to room temperature. The product was recovered from the flask and washed repeatedly with acetone. Purification was achieved by Soxhlet extraction using acetone for 24 hours, followed by drying in an oven at 70 °C to obtain solid hydrogel, which was then ground and characterized by FT-IR, TGA, swelling tests, rheology, and SEM.

Synthesis of DABCO-DMC ionic liquid. The DABCO–DMC ionic liquid was synthesized by heating a mixture of DABCO (0.202 g, 1.8 mmol) and DMC (9.72 g, 108 mmol) in a 1 : 6 molar ratio under reflux conditions for 5 hours. After the reaction, residual DMC was evaporated under reduced pressure using a rotary evaporator, yielding the final ionic liquid product (DABCO–DMC IL). ^{1}HNMR (400 MHz, DMSO-d6) δ 3.28 (t, J = 7.4 Hz, 6H), 3.17 (s, 3H), 3.02 (t, J = 7.5 Hz, 6H), 2.97 (s, 3H). ^{13}C NMR (75 MHz, DMSO-d6) 156, 53.6, 51.3, 49.1, 45.2. MS-ESI^{+}: 127.105 (100%), 128.098 (6.61%). Elemental analysis: C 53.45%, H 8.97; N 13.85%; Found C 53.56%, H 8.76%, N 13.7%.

Characterization

NMR. NMR spectra were acquired using a Bruker 400 AVANCE III HD instrument, outfitted with a BBI-z gradient probe head of 5 mm diameter. The test samples DABCO and DABCO ionic liquid were prepared by dissolving around 3 to 5 mg of the samples in deuterated DMSO (0.5 mL).

Mass spectra. ESI-MS investigations were carried out using a Thermo Fisher Scientific LCQ Advantage Max ion-trap mass spectrometer, which was equipped with an ESI source.

FTIR-ATR. The FTIR-ATR (Attenuated Total Reflection) analysis was performed using a PerkinElmer Spectrum 100 FT-IR Spectrometer (Waltham, MA, USA) fitted with a Universal ATR sampling accessory. The spectral data were acquired within the wavenumber range of 650–4000 cm^{-1} at ambient temperature. The instrument settings included a resolution of 4 cm^{-1} and an acquisition rate of 8 scans per spectrum.

TGA. Thermogravimetric analyses (TGA) were conducted on a TA Instruments Q500 TGA (New Castle, DE, USA) to investi-

gate the samples' behaviour. The experiments were performed under a nitrogen flow, from 50 °C to 500 °C, with a heating rate of 10 °C per minute.

CHNS elemental analysis. CHNS-elemental analysis (EA) is carried out to quantify accurate and reproducible carbon, hydrogen, nitrogen, and sulfur content in the synthesized polymers using a CHNS-O Analyser (Thermo Fisher Scientific FlashEA 1112 series; Waltham, MA, USA), equipped with Eager Xperience software (for Windows XP), and MAS 200R Auto Sampler. 2,5-Bis (5-*tert*-butyl-2-benzo-oxazol-2-yl) thiophene (BBOT) is used as an external standard for the calibration of the system. About 2.5 mg of each sample and an approximately equal quantity of V_2O_5 as a catalyst are placed in a tin container.

Scanning electron microscopy (SEM). Surface morphology analysis of the samples was performed using scanning electron microscopy. A Tescan VEGA 3 system (Brno, Czech Republic) equipped with secondary electron detection capabilities was employed for imaging, utilizing an acceleration voltage of 8 kV. To ensure optimal conductivity and minimize charging effects, all samples were pre-coated with a 12 nm gold layer using a Vac Coat DSR1 sputtering apparatus (London, UK) prior to SEM observation.

Water absorption capacity (WAC). The process of measuring water absorption capacity (WAC) involved placing 300 mg of dry powders into a 15 mL test tube containing deionized water, following a previously established protocol.[24] These test tubes were then sealed and left at room temperature. After 20 hours, the mixtures underwent centrifugation to separate the water-bound material from the unabsorbed water. Upon removal of the supernatant, the weight of the swollen polymer was noted. This procedure was repeated twice to ensure accuracy. The swelling rate, expressed as a percentage (% S) or the water absorption capacity (% WAC), was determined using eqn (1).

$$\mathrm{WAC} = \frac{m_t - m_0}{m_0} \times 100 \quad (1)$$

where m_t is the weight of the swollen sample and m_0 is the initial weight of the dry sample.

Cross-linking density determination using swelling experiments. The determination of cross-linking density through swelling experiments involves utilizing the water absorption capacity (WAC) data to calculate the polymer volume fraction in the equilibrium-swollen polymer (υ_{2m}). This fraction is then employed in the Flory–Rehner theory to derive the cross-linking density (υ). Cross-linking density (υ) refers to the number of cross-links per unit volume in a polymer network, while the polymer volume fraction indicates the amount of water that the polymer can absorb.

The M_c value is obtained using the Flory–Rehner equation, as represented by eqn (2):

$$M_c = \frac{V_1\left[(\upsilon_{2m})^{1/3} - \left(\frac{2}{f}\upsilon_{2m}\right)\right]}{-\left[\ln(1-\upsilon_{2m}) + \upsilon_{2m} + \chi_1(\upsilon_{2m})^2\right]} \quad (2)$$

In the provided context, χ_1 signifies the parameter for solvent-polymer interaction according to Flory–Huggins theory, V_1 represents the molar volume of water utilized for swelling, and f denotes the cross-link functionality. The relationship between M_c and υ is given by the following eqn (3):

$$M_c = \frac{\rho_p}{\upsilon} \quad (3)$$

Here, ρ_p represents the density of the polymer, which is accurately measured using a calibrated pycnometer. Cross-linking determination adhered to the methodology previously outlined by our research team,[24] with all measurements conducted in duplicate.

Mechanical properties (rheological measurements). Rheological analyses were conducted using a Rheometer TA Instruments Discovery HR 1, following the protocol outlined in previous research.[24,25] The instrument featured a 20 mm diameter stainless steel plate geometry and Peltier plate temperature control. Frequency sweep measurements ranged from 100 to 0.2 rad s^{-1}, with 5 points per decade, and a stress amplitude of 2%. An amplitude sweep test was employed to verify the stress amplitude value, ensuring measurements were within the linear viscoelastic region. Oscillatory shear mode was utilized to determine the shear modulus (G), including the storage modulus (G') and the loss modulus (G''), of the swollen polymers relative to frequency (Frequency Sweep test) and shear strain (Amplitude Sweep test). Samples were positioned between the upper parallel plate and a stationary surface with a 1 mm gap. A roughened surface geometry, such as a crosshatched plate, was utilized to enhance contact between the geometry and the sample.

The modulus measurements provide insight into the fraction of elastically effective network chains. The plateau modulus value $G'p$, determined through rheological measurements, correlates directly with the number of elastically effective chains per unit volume (υ_e), as indicated by eqn (4):

$$G'p = \left(1 - \frac{2}{f}\right) \times \upsilon_e \times RT \quad (4)$$

υ_e is the molar number of elastically effective network chains per unit volume estimated in mol m^{-3}, R is the universal gas constant (8.314 J mol^{-1} K^{-1}), T is the temperature, and f is the functionality formerly defined.

Theoretical simulations. Density Functional Theory (DFT) calculations were performed without applying molecular symmetry constraints on nuclear coordinates, using the ORCA 5.0.2 program package.[26] The B3LYP functional[27] with D3BJ dispersion correction[28] and Pople's 6-311++G(d,p) split-valence basis set[29] was employed. All stationary points were confirmed as minima. Molecular structures were visualized using ChemCraft software.[30]

Results and discussion

Covalently cross-linked hydrogels derived from GLU2 were successfully synthesized with a high yield of approximately 80%, as shown in Scheme 2, through transesterification of GLU2

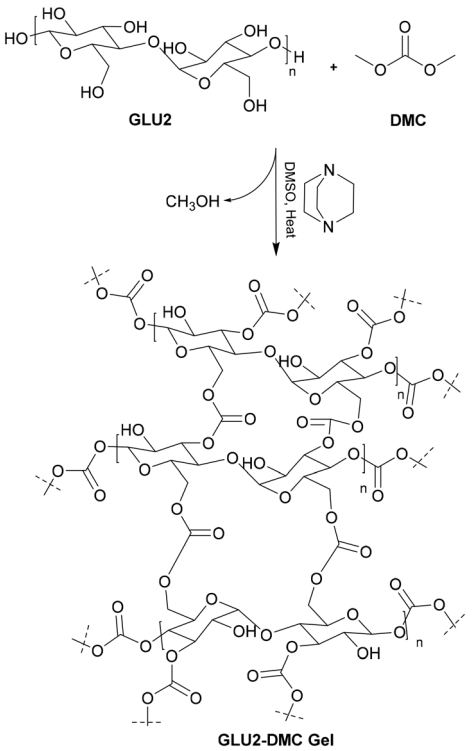

Scheme 2 Synthesis of GLU2-DMC hydrogel.

with DMC. The synthesis was carried out under mild reaction conditions using DABCO as an organocatalyst and DMSO as the solvent. This method adheres to the principles of green chemistry, particularly due to the choice of DMSO, which is a less toxic solvent compared to conventional alternatives. The use of DMSO not only minimizes toxicity but also contributes to the sustainability of the process compared to conventional alternatives to prepare carbonated maltodextrin covalently crosslinked polymers and hydrogels (Scheme 1).

For comparison, Trotta *et al.*[31] demonstrated in their patent the preparation of maltodextrin-carbonate cross-linked polymers using traditional crosslinkers such as diphenylcarbonate (DPC), *N*,*N*'-carbonyldiimidazole (CDI), and triphosgene (TP). However, it is important to note that while the method using DPC was described in detail in their patent, the methods for TP and CDI were not explicitly mentioned. The methods for these crosslinkers appear to have been inferred from similar reactions in the literature.[32–34] Specifically, Trotta *et al.*'s patent focused on the use of DPC, to prepare carbonate-based polymers for drug delivery systems using cyclodextrins, with triethylamine as the catalyst and DMF as the solvent for 3 hours.[31] Similarly, TP has been used for the synthesis of linear polycarbonates in a biphasic system of water and DCM at 60 °C with NaOH as the catalyst.[35] These methods, although effective, involve toxic reagents and harsh conditions, making them less sustainable. In contrast, the preparation of covalently cross-linked maltodextrin-based hydrogels in the literature often involves radical polymerization. This process is carried out in two steps: first, maltodextrin is functionalized with glycidyl methacrylate (GMA) to introduce acrylic groups, followed by radical polymerization with acrylic monomers to form cross-linked hydrogels. However, these methods tend to require toxic reagents such as GMA, acrylic acid, and acrylamide, in addition to radical initiators, which makes them more expensive and less environmentally friendly. For instance, Meléndez-Ortiz *et al.*[15] synthesized maltodextrin-based cross-linked hydrogels by first functionalizing maltodextrin with GMA in the presence of HCl, followed by free radical polymerization with either acrylic acid (AAc) or acrylamide (AAm) at 60 °C for 4 hours. The GMA-functionalized maltodextrin undergoes polymerization, introducing methacrylic groups that enable cross-linking. Moreover, Paulino *et al.*[36] prepared a maltodextrin-based hydrogel using a similar functionalization route with GMA, which undergoes either an epoxy ring-opening mechanism or transesterification, producing glycidol as a byproduct. This was followed by radical polymerization. Similarly, Meléndez-Ortiz *et al.*[37] and Guilherme *et al.*[38] made slight modifications to the process, replacing acrylic acid or acrylic monomers with vinyl-functionalized mineral crosslinkers or *n*,*n*-dimethylacrylamide, which were then cross-linked through radical polymerization. In contrast to these more complex and toxic methods, our approach offers a greener and more sustainable alternative by using dimethylcarbonate (DMC) as the crosslinking agent, DMSO as the solvent, and DABCO as the catalyst. DMC, a well-known environmentally friendly reagent, provides a non-toxic and biodegradable alternative to phosgene-based crosslinkers such as TP and CDI.

This is an important advantage, as DMC's use significantly reduces the environmental and health risks associated with toxic reagents like phenol, imidazole, and triphosgene. Furthermore, DMSO, a biodegradable, non-halogenated solvent, is used in place of DMF and DCM, which are associated with higher toxicity and environmental concerns.[39–42] While DMC as carbonate source does produce methanol as a byproduct which is fully degradable,[43] it is comparatively safer to handle than phenol or imidazole, and it is easier to manage than chlorinated byproducts as from a green chemistry perspective, methanol emerges as the most favorable byproduct due to its relatively low environmental persistence, minimal ecotoxicological impact, and feasibility of recovery/recycling, whereas phenol is the least desirable owing to its high toxicity, bioaccumulative potential, and challenges in remediation, with imidazole presenting an intermediate profile due to variable degradability and risks associated with nitrogenous pollution.[1,43–55] Our method not only provides a sustainable alternative to existing practices but also simplifies the synthesis procedure, avoids the use of toxic reagents, and minimizes waste production, making it a more environmentally friendly approach to preparing maltodextrin-based cross-linked hydrogels. Furthermore, the substitution of dimethyl carbonate for diphenyl carbonate aligns with environmental sustainability goals, mitigating the release of phenol into the environment. Notably, the enhanced atom economy of

dimethyl carbonate contributes to its favourable ecological profile. The vital role of DABCO in facilitating transesterification reactions within the hydrogel synthesis process was investigated. Variation in the molar ratio of DABCO, ranging from 1.8 mmol to 0.152 mmol, yielded insights into its impact on reaction kinetics. It was observed that diminishing the concentration of DABCO correlated with prolonged transesterification times, extending from 30 minutes at 1.8 mmol to 5 hours using 0.152 mmol, to achieve the desired formation of non-soluble hydrogels, as delineated in Table 1. Subsequently, experiments conducted under a reduced DABCO molar ratio of 0.107 mmol revealed a notable absence of non-soluble hydrogel formation, even after an extended reaction duration of 3 days.

Various solvents, including Dimethylformamide (DMF), Tetrahydrofuran (THF), Acetone, and Acetonitrile (MeCN), were assessed alongside DMSO. The crosslinking of maltodextrin with DMC in the presence of DABCO as a catalyst to form non-soluble hydrogels was successful exclusively in DMSO, highlighting the solvent's critical role in the reaction. DMSO's high polarity and dipolar aprotic nature stabilize the ionic liquid formed between DABCO and DMC, as confirmed by NMR spectra in DMSO, enabling the activation of DMC and efficient crosslinking. Unlike other solvents, DMSO dissolves maltodextrin and stabilizes ionic intermediates without introducing competing hydrogen-bonding interactions, ensuring a clean reaction pathway and minimizing side reactions. This selectivity underscores the importance of solvent properties, as less polar or protic solvents failed to facilitate the reaction due to inadequate stabilization of the ionic species.[56] While DMSO is a synthetic solvent, its role in enabling ionic liquid-mediated transformations under mild and efficient conditions aligns with green chemistry principles by reducing waste and avoiding harsh reagents. These findings highlight DMSO's unique capacity to promote sustainable and effective hydrogel synthesis. Different molar ratios of DMC were used as crosslinking units Table 2, starting from 8.6 (475.14 mmol), 4.3 (237.6 mmol), 2.15 (118.8 mmol), 1.08 (59.4 mmol), 0.5 (29.8 mmol), and 0.3 (14.8 mmol) molar equivalents to each glucose unit in GLU2. These were utilized at 85 °C to perform the hydrogel formation. It was observed that as the molar ratio of DMC decreased, the reaction time until the formation of hydrogels increased, ranging from 0.17 hours to 6 hours for a 0.3 molar ratio of DMC. Below this ratio, there was no formation of hydrogels even after leaving the reaction for 3 days at 85 °C. This indicates that a 1 : 3 molar ratio of DMC to glucose units in the maltodextrin polymer is necessary. The reaction yields were around 80%, with corresponding reaction times of 0.17, 0.25, 0.45, 1.00, 1.50, and 6 hours, respectively as shown in Table 1.

To examine the temperature influence Table 3, adjustments were made from 70 °C to 110 °C. Decreasing the temperature to (70 °C) resulted in a prolonged reaction time of 1.50 hours, compared to the 0.50-hour reaction time at 85 °C. Conversely, elevating the temperature to 110 °C remarkably shortened the reaction time to 0.25 hours giving that the boiling point on DMC is 95 °C due to the reflux system. Interestingly, altering the temperature did not noticeably impact the yield.

The hydrogel synthesized at 85 °C exhibited the highest swelling capacity and was selected as the optimal formulation for this investigation. As shown in Fig. 1, the surface morphology and microstructure of the hydrogel reveal porous features and distinct qualitative differences compared to the

Table 1 Effect of DABCO molar ratio on reaction time and yield at a constant reaction temperature of 85 °C, Maltodextrin 5.55 mmol and DMC 118.8 mmol

Entry	DABCO (mmol)	Time (h)	Yield (%)
1	1.8	0.45	83
2	0.893	0.45	80
3	0.669	1.25	83
4	0.445	1.50	78
5	0.223	2.00	79
6	0.178	3.25	81
7	0.152	5.00	78
8	0.107	48.00	ND
9	0	48.00	ND

Table 2 Effect of DMC molar ratio on reaction time and yield at a constant reaction temperature of 85 °C, Maltodextrin 5.55 mmol and DABCO 1.8 mmol

Entry	DMC (mmol)	Time (h)	Yield (%)
1	475.14	0.17	80
2	237.6	0.25	79
3	118.8	0.45	83
4	59.4	1	81
5	29.8	1.5	82
6	14.9	6	80

Table 3 Effect of Temperature on reaction time and yield using Maltodextrin 5.55 mmol, DABCO 0.892 mmol and DMC 118.8 mmol

Entry	Temperature (°C)	Time (h)	Yield (%)
1	70	1.50	83
2	85	0.45	82
3	110	0.25	80

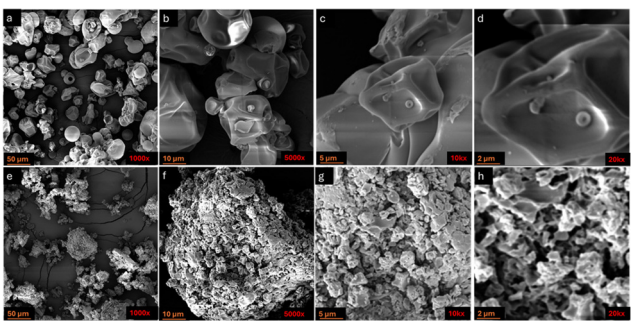

Fig. 1 SEM images of GLU2 (a–d) and GLU2 hydrogel synthesized at 85 °C using 100 mg(0.892 mmol) of DABCO (e–h) as it is after synthesis and drying in oven at 70 °C.

GLU2 starting material, which lacks porosity. The micro-roughness observed in the hydrogel is advantageous for tissue engineering applications, as it supports cellular attachment, proliferation, and tissue development within the scaffolds.[57] Furthermore, we explored the impact of various drying methods on pore structure. Our findings indicate that freeze-drying preserved larger pores, while oven-drying produced smaller pores without structural collapse. Conversely, air-drying resulted in no detectable pores, as shown in Fig. 5S in the ESI.† These results highlight how post-synthesis drying techniques can dictate pore size.

Fig. 2a and b displays the FTIR spectra for the maltodextrin carbonate hydrogels, highlighting samples prepared with varying DABCO molar ratios and reaction temperatures. All synthesized hydrogels show a distinct absorption band near 1750 cm^{-1}, which is indicative of the carbonyl group associated with the carbonate bond. This band is absent in the starting GLU2 precursor, thereby confirming the successful incorporation of carbonate functionalities under the used green chemistry conditions. The TGA analysis in Fig. 2c and d shows that the hydrogels remained thermally stable up to approximately 200 °C, while degradation occurred in a two-step process roughly between 200 °C and 400 °C, resulting in a stable carbon residue at 500 °C, approximately corresponding to 15% of the initial weight.

Fig. 3a and as indicated in Table 1S in the ESI† displays the effect of catalyst amount in water absorption capacity (WAC). By increasing the amount of DABCO catalyst from 50 mg (0.445 mmol) to 75 mg (0.669 mmol) the WAC decreases from 468% to 400%, whereas for the amount of 100 mg (0.892 mmol) DABCO, the WAC was 460% as presented. It is observed a slight difference when the amount of catalyst changes. Furthermore, Fig. 3b, as reported in Table 1S in the ESI†, presents the effect of temperature in WAC. If temperature increases from 70 °C to 85 °C, the WAC increases to 549%.

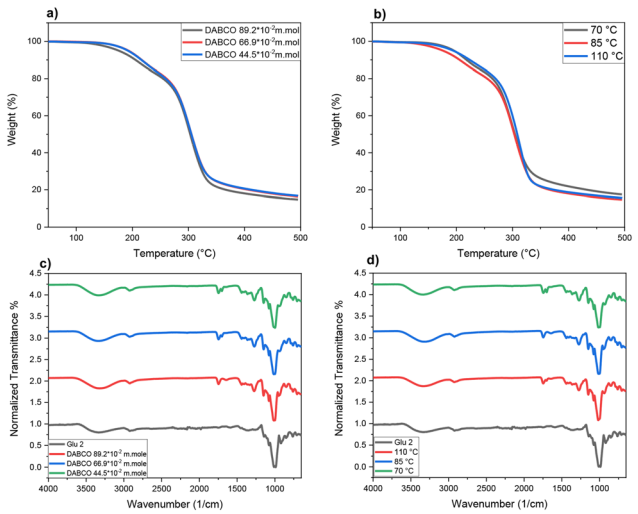

Fig. 2 TGA and FT-ATIR of the crosslinked hydrogels using different molar ratio of DABCO l and at different reaction temperatures.

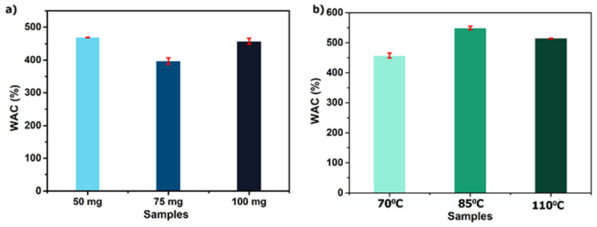

Fig. 3 (a) changing the amount of catalyst ((50 mg (0.445 mmol), 75 mg (0.669 mmol), and 100 mg (0.892 mmol)); and b) various temperature conditions (70, 85, and 110 °C).

Whereas the further increasing of the reaction temperature results in a slight decrease of WAC as illustrated in Table 1S in the ESI.† This suggests that higher catalyst concentrations initially promote crosslinking, reducing water uptake, but beyond a certain threshold, the network may become more hydrophilic, allowing for increased water absorption.

The Flory–Rehner equation (eqn (2)) is a foundational model in polymer science that quantifies the mixing behaviour between polymer chains and solvent molecules. Based on the equilibrium swelling theory proposed by Flory and Rehner,[58] the equation links the degree of swelling in lightly crosslinked polymers to both the density of crosslinks and the solvent's quality. This relationship provides valuable insights into the thermodynamic interactions governing polymer swelling, facilitating a deeper understanding of how structural factors influence material behaviour.

Fig. 4a illustrates that the cross–linking density—calculated using the Flory–Rehner theory—increases systematically with the DABCO catalyst concentration, using 50 mg (0.445 mmol), 75 mg (0.669 mmol), and 100 mg (0.892 mmol) doses. This trend indicates that augmenting the DABCO content substantially modifies the network structure by enhancing the cross–linking process. Moreover, as shown in Fig. 4b, the effect of synthesis temperature on the cross–linking density is non–linear. Initially, an increase in temperature from 70 °C to 85 °C leads to a reduction in cross–linking density, suggesting potential network relaxation or side reactions that temporarily reduce cross–link formation. However, when the synthesis temperature is further increased to 110 °C, a marked increase in cross–linking density is observed, implying that higher

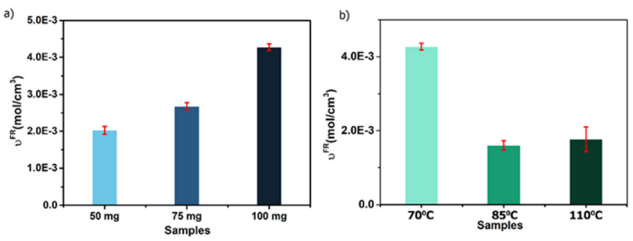

Fig. 4 Cross-linking density determined by Flory–Rehner theory (υ^{FR}) of samples synthesized by (a) changing the amount of catalyst ((50 mg (0.445 mmol), 75 mg (0.669 mmol), and 100 mg (0.892 mmol)); and b) various temperature conditions (70, 85, and 110 °C).

thermal energy overcomes these intermediate effects to favour enhanced network formation. Overall, these findings highlight the critical roles of both catalyst concentration and synthesis temperature in tuning the cross–linked network properties.

The mechanical performance of the hydrogels was further examined. The results indicate that the storage modulus (G') remained nearly constant for all hydrogels, while the loss modulus (G'') exhibited a modest increase with rising angular frequency (ω) (Fig. 5 and 6) and as illustrated in Table 1S in the ESI.† Moreover, the storage modulus consistently exceeded the loss modulus. Stable covalent hydrogels formed due to the presence of chemical linkages, while the increase of the G' and G'' with frequency and closeness in the value at the upper frequency range are due to the coexistence of physical interaction. Multiple cross-linking induces a flexible property in hydrogels, which enables them to dissipate energy under application of frequency. Thus, integrating rheological models—which evaluate the storage modulus (G', reflecting elastic solid-like behaviour) and loss modulus (G'', capturing viscous liquid-like response) with the Flory–Rehner equation (governing swelling thermodynamics) provides a dual analytical framework. This approach enables simultaneous characterization of both the swelling dynamics, dictated by solvent-polymer interactions, and the mechanical robustness of crosslinked polymer systems.

We observed that increasing the DABCO catalyst amount beyond 75 mg led to a decrease in effective sub-chain density (υ_e^R), as determined by rheological measurements (Fig. 7a). This suggests that excessive catalyst amounts may disrupt network structure, reducing the number of effective sub-chains per unit volume. Conversely, synthesizing samples at 110 °C resulted in the highest cross-linking density (Fig. 7b), indicating that elevated temperatures promote enhanced network formation. These findings highlight the importance of optimizing synthesis parameters to tailor hydrogel properties for specific applications.

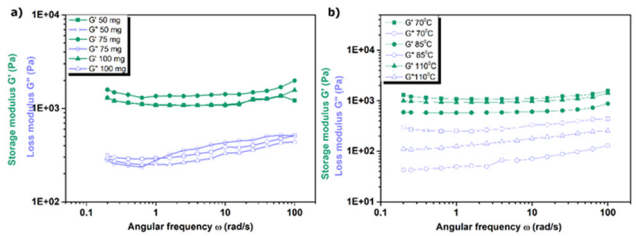

Fig. 5 Storage (G') and loss (G'') modulus *versus* angular frequency for samples synthesized by (a) changing the amount of catalyst ((50 mg (0.445 mmol), 75 mg (0.669 mmol), and 100 mg (0.892 mmol)); and b) various temperature conditions (70 °C, 85 °C, and 110 °C).

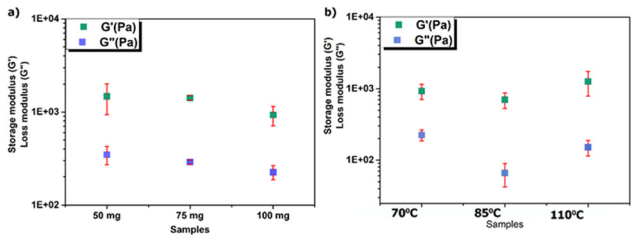

Fig. 6 Storage (G') and loss (G'') modulus for samples synthesized (a) changing the amount of catalyst ((50 mg (0.445 mmol), 75 mg (0.669 × 10^{-3} mmol), and 100 mg (0.892 mmol)); and b) various temperature conditions (70 °C, 85 °C, and 110 °C) at an angular frequency (ω) of 1 rad s^{-1}.

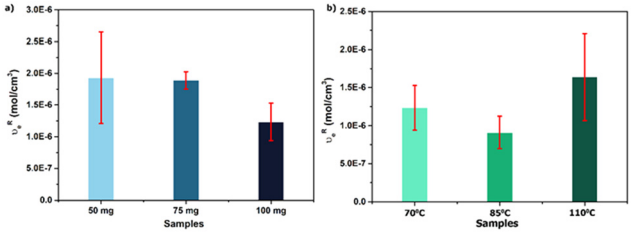

Fig. 7 Effective sub-chain density (moles of effective sub-chains per unit volume) determined by rheology (υ_e^R) of samples synthesized by (a) changing the amount of catalyst ((50 mg (0.445 mmol), 75 mg (0.669 mmol), and 100 mg (0.892 mmol)); and (b) various temperature conditions (70 °C, 85 °C, and 110 °C).

Molecular weight between crosslinks (M_c) in ESI (Table 1S)† decreased from 494 ± 26 g mol^{-1} at 50 mg to 234 ± 5 g mol^{-1} at 100 mg, highlighting that increased catalyst concentrations facilitate the formation of a denser crosslinked network with shorter polymer segments between crosslinks. The observed variations in – M_c across different synthesis temperatures—234 ± 5 g mol^{-1} at 70 °C, 629 ± 51 g mol^{-1} at 85 °C, and 578 ± 110 g mol^{-1} at 110 °C—suggest a complex interplay between temperature and hydrogel network formation. Typically, increasing synthesis temperature enhances the reactivity of monomers and crosslinking agents, leading to a more interconnected network and a decrease in M_c. However, the data here indicate that the effect of temperature on M_c is not linear. At 85 °C, the M_c value peaks, possibly due to optimal crosslinking efficiency or changes in polymerization kinetics. At 110 °C, while one might expect a further increase in M_c, the observed slight decrease could be due to higher temperatures that can accelerate polymerization rates, potentially leading to a more densely crosslinked network and shorter polymer segments between crosslinks, resulting in a lower M_c value.

Mechanism

DABCO, known for its nucleophilic base properties, is widely utilized as a catalyst in various reactions, including esterification reactions. Based on these established applications, we explored the potential of DABCO as a catalyst for the transesterification of GLU2 with DMC to obtain maltodextrin crosslinked hydrogels.[59–61] Drawing from the mechanism proposed for the *N*-methylation of indole with DMC using DABCO as a catalyst, it is suggested that DMC undergoes activation by DABCO, leading to the formation of an ion pair.[59] This ion pair facilitates efficient *N*-methylation of indole and is regenerated by the nucleophilic attack of DABCO on DMC. To verify

this, we attempted the synthesis of DABCO–DMC IL as reported in the experiential part. The obtained ^{1}H NMR in DMSO-d_6 results as shown in Fig. 1S in the ESI,† revealed the formation of ionic liquids as after 40 minutes, with MS-ESI^{+} Fig. 2S in ESI† confirming the presence of ionic liquid and DABCO giving the exact mass of the counter methylated DABCO ion and to confirm the presence of counter ion we performed the ^{13}C NMR as illustrated in Fig. 3S in the ESI† which matches the ionic-liquid and the carbonyl carbon of the negative ion is present at 156 ppm chemical shift. The proposed mechanism involving two main steps: the formation of DABCO–DMC ionic liquid (IL) and the subsequent synthesis of GLU2 crosslinked hydrogels using this IL as a catalyst. In the first step, DABCO acts as a nucleophilic catalyst, reacting with DMC to form an ion pair, resulting in the less basic DABCO–DMC IL (Scheme 2).[59,62] Despite the pH difference between DABCO and DABCO–DMC IL, the enhanced activity observed with DABCO–DMC IL suggest a role beyond basicity, likely involving both cations and anions in hydrogel formation. Prior research indicates rare instances of ILs catalysing reactions through combined cation and anion activation.[63] Hence, a proposed mechanism (Scheme 3) depicts both cation and anion playing crucial roles in the one-pot synthesis of GLU2 hydrogel from GLU2 and DMC. The nitrogen–oxygen interaction facilitates the coordination of the IL's N centre to DMC's carbonyl oxygen, activating DMC. Nucleophilic activation may occur through anion-proton exchange with GLU2, leading to GLU2-oxide formation (GLU2 activation). Following catalyst-triggered electrophile and nucleophile activation, GLU2-oxide attacks the activated carbonyl carbon, yielding GLU2 methyl carbonate (intermediate, Structure **A**). Subsequent reactions and crosslinking of GLU2 methyl carbonate lead to hydrogel formation, completing transesterification.

The primary objective of quantum-chemical simulations in this study is to evaluate charge redistribution between reagents and the distances between interacting atoms during the reaction. The initial stage of crosslinked hydrogel formation involves the generation of the DABCO-DMC ionic pair. The interaction between the DABCO molecule and DMC induces electron redistribution, supporting the hypothesis of DABCO's nucleophilic role (Fig. 8a). Specifically, the Löwdin atomic charges of the nitrogen atom in DABCO and the oxygen atom in DMC decrease by approximately 0.02 e. Furthermore, the Mayer bond order of the C–O bond in DMC significantly

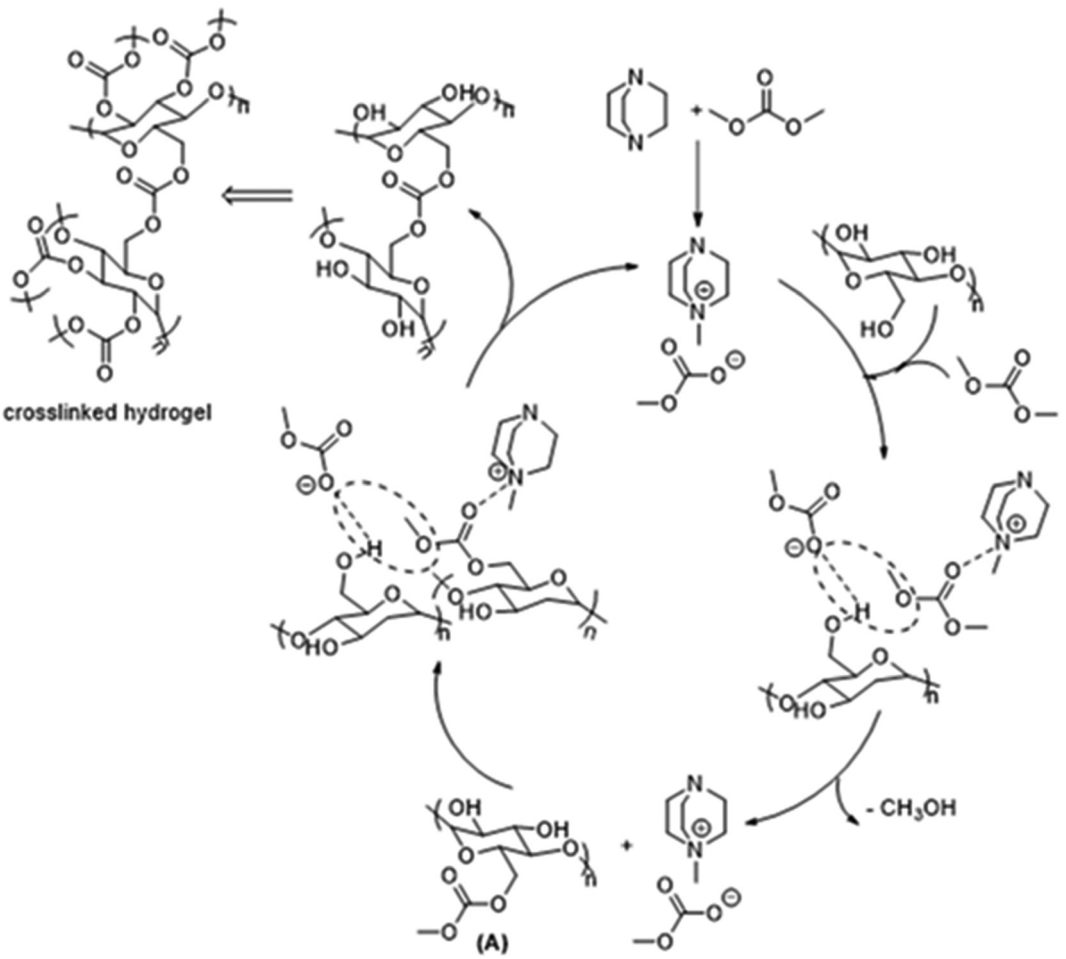

Scheme 3 Proposed mechanism for the formation of crosslinked hydrogel.

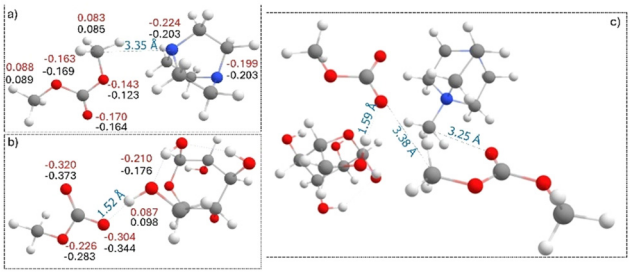

Fig. 8 Geometry of the optimized structures of the DABCO-DMC ionic pair (a), glucose and methylcarbonate anion (b), and the initial polymer reaction compounds (c), carbon, hydrogen, oxygen, and nitrogen atoms are represented in gray, white, red, and blue, respectively. Selected interatomic distances are shown in blue. Löwdin atomic charges are indicated in black for isolated compounds and in red for interacting compounds.

decreases from 1.13 to 0.8 upon interaction with DABCO, confirming the feasibility of DABCO-DMC ionic liquid formation. Another key interaction in the studied reaction is between GLU2 and the DMC anion. To model this interaction, GLU2 was simplified using a glucose molecule. One of the hydroxyl hydrogen atoms in glucose forms a hydrogen bond with an oxygen atom in the DMC anion (Fig. 8b) at a distance of 1.52 Å. Following this interaction, the oxygen atoms in the DMC anion become more positively charged, whereas the oxygen atom in glucose becomes more negatively charged. The spatial arrangement of all interacting compounds in the crosslinked hydrogel reaction is depicted in Fig. 8c. The hydrogen bond persists but at a slightly greater distance (1.59 Å). The distance between the carboxyl oxygen atom in DMC and the carbon from the CH_3 group of the DABCO cation measures 3.25 Å, while the distance between the CH_3 group of the DMC molecule and the DMC anion is 3.38 Å. This spatial reorganization, along with electronic redistribution, facilitates the release of a CH_3OH molecule that proves proposed mechanism in Scheme 3.

Conclusions

This work demonstrates a sustainable, one-pot synthesis of 10 gram scale maltodextrin-based hydrogels using DMC as a phosgene-free crosslinker, DABCO as a non-toxic organocatalyst, and DMSO as a biodegradable solvent. The method adheres to green chemistry principles, achieving an impressive 80% yield under mild conditions (70–110 °C). The hydrogels exhibit tunable crosslinking densities (as described by Flory–Rehner theory), high water absorption capacity (up to 549%), and robust viscoelastic properties ($G' > G''$), making them ideal for biomedical applications. By replacing hazardous reagents (*e.g.*, phenol, DMF, acrylamide) and energy-intensive steps with eco-friendly alternatives, this strategy advances scalable, low-impact polymer synthesis, aligning with global efforts toward sustainable material design. Compared to existing methods, the presented synthesis offers a more sustainable and efficient route to hydrogel formation, highlighting its potential for future applications in areas such as environmental remediation and biomedical materials in drug delivery systems, tissue engineering, agriculture, food industry, *etc*. While application studies fall beyond the current scope, the fundamental advances reported here lay a solid foundation for such developments.

Author contributions

Mohamed M. H. Desoky: conceptualization, investigation, methodology, writing – original draft. G. Hotti: investigation, methodology, and writing. A. Tsaturyan: investigation, methodology, and writing. C. Cecone: investigation. F. Caldera: writing – review. F. Trotta: conceptualization, writing – review, funding and acquisition, and supervision. The manuscript was reviewed by all authors.

Conflicts of interest

Ther is no conflict of interest.

Data availability

All supporting data are available at ESI.†

Acknowledgements

Authors acknowledge support from the Project CH4.0 under the MUR program "Dipartimenti di Eccellenza 2023–2027" (CUP: D13C22003520001). A. T. acknowledges for financially support the Ministry of Science and Higher Education of the RF in the framework of the State assignment in the field of scientific activity No. FENW_2023-0020.

References

1 P. T. Anastas and J. C. Warner, *Green Chemistry: Theory and Practice*, Oxford University Press, 1998.
2 X. Huang and T. L. Lowe, *Biomacromolecules*, 2005, **6**, 2131–2139.
3 L. Chafran, A. Carfagno, A. Altalhi and B. Bishop, *Polymers*, 2022, **14**, 4755.
4 D. D. Sun and P. I. Lee, *Acta Pharm. Sin. B*, 2014, **4**, 26–36.
5 N. Vyavahare and J. Kohn, *J. Polym. Sci., Part A: Polym. Chem.*, 1994, **32**, 1271–1281.
6 M. Ishihara, K. Ono, M. Sato, K. Nakanishi, Y. Saito, H. Yura, T. Matsui, H. Hattori, M. Fujita, M. Kikuchi and A. Kurita, *Wound Repair Regen.*, 2001, **9**, 513–521.
7 J. L. Drury and D. J. Mooney, *Biomaterials*, 2003, **24**, 4337–4351.

8 T. Chen, H. D. Embree, E. M. Brown, M. M. Taylor and G. F. Payne, *Biomaterials*, 2003, **24**, 2831–2841.
9 N. Peppas, *Eur. J. Pharm. Biopharm.*, 2000, **50**, 27–46.
10 1998, pp. i–vi.
11 H. M. El-Husseiny, E. A. Mady, L. Hamabe, A. Abugomaa, K. Shimada, T. Yoshida, T. Tanaka, A. Yokoi, M. Elbadawy and R. Tanaka, *Mater. Today Bio*, 2022, **13**, 100186.
12 G. Hoti, R. Ferrero, F. Caldera, F. Trotta, M. Corno, S. Pantaleone, M. M. H. Desoky and V. Brunella, *Polymers*, 2023, **15**, 1543.
13 O. Okay and Ç. Gürün, *J. Appl. Polym. Sci.*, 1992, **46**, 401–410.
14 J.-P. Draye, B. Delaey, A. Van de Voorde, A. Van Den Bulcke, B. Bogdanov and E. Schacht, *Biomaterials*, 1998, **19**, 99–107.
15 H. I. Meléndez-Ortiz, R. Betancourt-Galindo, B. Puente-Urbina, A. Ledezma and O. Rodríguez-Fernández, *Int. J. Polym. Mater. Polym. Biomater.*, 2021, **71**, 959–968.
16 A. Jain, S. K. Prajapati, A. Kumari, N. Mody and M. Bajpai, *J. Drug Delivery Sci. Technol.*, 2020, **57**, 1–18.
17 A. Parikh, S. Agarwal and K. R. Department, *Int. J. Drug Dev. Res.*, 2014, **4**, 67–74.
18 Z. Xiao, J. Xia, Q. Zhao, Y. Niu and D. Zhao, *Carbohydr. Polym.*, 2022, **298**, 120113.
19 J. Wu, X. Sun and Y. Li, *Eur. J. Org. Chem.*, 2005, **2005**, 4271–4275.
20 K. Yamguchi, M. Eto, K. Higashi, Y. Yoshitake and K. Harano, *Tetrahedron Lett.*, 2011, **52**, 6082–6085.
21 N. Chakraborty and A. K. Mitra, *Org. Biomol. Chem.*, 2023, **21**, 6830–6880.
22 F. S. H. Simanjuntak, J. S. Choi, G. Lee, H. J. Lee, S. D. Lee, M. Cheong, H. S. Kim and H. Lee, *Appl. Catal., B*, 2015, **165**, 642–650.
23 N. Singh and J. Pandey, *Curr. Res. Green Sustain. Chem.*, 2021, **4**, 100134.
24 G. Hoti, F. Caldera, C. Cecone, R. A. Pedrazzo, A. Anceschi, S. L. Appleton, Y. K. Monfared and F. Trotta, *Materials*, 2021, **14**, 478.
25 G. Hoti, F. Caldera, C. Cecone, A. R. Pedrazzo, A. Anceschi, S. L. Appleton, Y. K. Monfared and F. Trotta, *Materials*, 2021, **14**, 1–20.
26 F. Neese, F. Wennmohs, U. Becker and C. Riplinger, *J. Chem. Phys.*, 2020, **152**, 224108.
27 A. D. Becke, *J. Chem. Phys.*, 1993, **98**, 5648–5652.
28 S. Grimme, S. Ehrlich and L. Goerigk, *J. Comput. Chem.*, 2011, **32**, 1456–1465.
29 W. J. Hehre, R. Ditchfield and J. A. Pople, *J. Chem. Phys.*, 1972, **56**, 2257–2261.
30 ChemCraft, version 1.6, ChemCraft -, *Graphical Software for Visualization of Quantum Chemistry Computations*, 2008, **https://www.chemcraftprog.com**.
31 F. Trotta and E. Fossati, *WO Pat.*, WO2016004974A1, 2016.
32 M. K. Anwer, M. M. Ahmed, M. F. Aldawsari, M. Iqbal and V. Kumar, *Pharmaceuticals*, 2022, **16**, 19.
33 M. F. Aldawsari, A. H. Alhowail, M. K. Anwer and M. M. Ahmed, *Int. J. Nanomed.*, 2023, **18**, 2239–2251.
34 W. B. Liechty and N. A. Peppas, *Eur. J. Pharm. Biopharm.*, 2012, **80**, 241–246.
35 Y. E, P. Lv and F. Yang, *J. Phys.: Conf. Ser.*, 2022, **2194**, 012033.
36 A. T. Paulino, A. R. Fajardo, A. P. Junior, E. C. Muniz and E. B. Tambourgi, *Polym. Int.*, 2011, **60**, 1324–1333.
37 H. I. Meléndez-Ortiz, R. Betancourt-Galindo, B. Puente-Urbina, J. L. Sánchez-Orozco and A. Ledezma, *Int. J. Biol. Macromol.*, 2022, **198**, 119–127.
38 M. R. Guilherme, A. R. Fajardo, T. A. Moia, M. H. Kunita, M. C. Gonçalves, A. F. Rubira and E. B. Tambourgi, *Eur. Polym. J.*, 2010, **46**, 1465–1474.
39 S. Hong, X. Zhang, Z. Sun and T. Zeng, *J. Appl. Toxicol.*, 2024, **44**, 1637–1646.
40 J. P. Rioux and R. A. M. Myers, *J. Emerg. Med.*, 1988, **6**, 227–238.
41 F. P. Byrne, S. Jin, G. Paggiola, T. H. M. Petchey, J. H. Clark, T. J. Farmer, A. J. Hunt, C. R. McElroy and J. Sherwood, *Sustainable Chem. Processes*, 2016, **4**, 1–24.
42 R. D. Nyamiati, Y. Rahmawati, A. Altway and S. Nurkhamidah, *IOP Conf. Ser.:Mater. Sci. Eng.*, 2021, **1143**, 012063.
43 C. J. C. Van De Ven, L. Laurenzi, A. C. Arnold, S. J. Hallam and K. U. Mayer, *J. Contam. Hydrol.*, 2022, **247**, 103988.
44 P. I. Nikel, D. Pérez-Pantoja and V. de Lorenzo, *Philos. Trans. R. Soc., B*, 2013, **368**, 20120377.
45 L. Cotarca, T. Geller and J. Répási, *Org. Process Res. Dev.*, 2017, **21**, 1439–1446.
46 N. Panigrahy, A. Priyadarshini, M. M. Sahoo, A. K. Verma, A. Daverey and N. K. Sahoo, *Environ. Technol. Innovation*, 2022, **27**, 102423.
47 W. de Vries, *Curr. Opin. Environ. Sci. Health*, 2021, **21**, 100249.
48 A. Dodangeh, M. M. Rajabi, J. Carrera and M. Fahs, *J. Contam. Hydrol.*, 2022, **247**, 103980.
49 J. Sun, Q. Mu, H. Kimura, V. Murugadoss, M. He, W. Du and C. Hou, *Adv. Compos. Hybrid Mater.*, 2022, **5**, 627–640.
50 S. Evjen, O. A. H. Åstrand, M. Gaarder, R. E. Paulsen, A. Fiksdahl and H. K. Knuutila, *Ind. Eng. Chem. Res.*, 2020, **59**, 587–595.
51 A. Hussain, *Int. J. Environ. Eng.*, 2014, **1**, 151–157.
52 R. P. Schwarzenbach, B. I. Escher, K. Fenner, T. B. Hofstetter, C. A. Johnson, U. von Gunten and B. Wehrli, *Science*, 2006, **313**, 1072–1077.
53 J. Kim and N. Armstrong, *Water Res.*, 1981, **15**, 1233–1247.
54 Z. Yu and E. R. Bernstein, *J. Phys. Chem. A*, 2013, **117**, 1756–1764.
55 D. Spasiano, A. Siciliano, M. Race, R. Marotta, M. Guida, R. Andreozzi and F. Pirozzi, *Water Res.*, 2016, **106**, 450–460.
56 T. A. Bioni, M. L. de Oliveira, M. T. Dignani and O. A. El Seoud, *New J. Chem.*, 2020, **44**, 14906–14914.
57 S. Kyle, Z. M. Jessop, A. Al-Sabah, K. Hawkins, A. Lewis, T. Maffeis, C. Charbonneau, A. Gazze, L. W. Francis, M. Iakovlev, K. Nelson, S. J. Eichhorn and I. S. Whitaker, *Carbohydr. Polym.*, 2018, **198**, 270–280.
58 P. J. Flory and J. Rehner, *J. Chem. Phys.*, 1943, **11**, 521–526.

59 W.-C. Shieh, S. Dell, A. Bach, O. Repič and T. J. Blacklock, *J. Org. Chem.*, 2003, **68**, 1954–1957.
60 C. Yu, B. Liu and L. Hu, *J. Org. Chem.*, 2001, **66**, 5413–5418.
61 J. A. Linn, E. W. McLean and J. L. Kelley, *J. Chem. Soc., Chem. Commun.*, 1994, 913.
62 S. M. Gade, M. K. Munshi, B. M. Chherawalla, V. H. Rane and A. A. Kelkar, *Catal. Commun.*, 2012, **27**, 184–188.
63 A. K. Chakraborti and S. R. Roy, *J. Am. Chem. Soc.*, 2009, **131**, 6902–6903.